

APPLICATIONS OF NONLINEAR DIFFUSION IN IMAGE PROCESSING AND COMPUTER VISION

J. WEICKERT

ABSTRACT. Nonlinear diffusion processes can be found in many recent methods for image processing and computer vision. In this article, four applications are surveyed: nonlinear diffusion filtering, variational image regularization, optic flow estimation, and geodesic active contours. For each of these techniques we explain the main ideas, discuss theoretical properties and present an appropriate numerical scheme. The numerical schemes are based on additive operator splittings (AOS). In contrast to traditional multiplicative splittings such as ADI, LOD or D'yakonov splittings, all axes are treated in the same manner, and additional possibilities for efficient realizations on parallel and distributed architectures appear. Geodesic active contours lead to equations that resemble mean curvature motion. For this application, a novel AOS scheme is presented that uses harmonic averaging and does not require reinitializations of the distance function in each iteration step. Its accuracy is evaluated in case of mean curvature motion.

1. INTRODUCTION

Many mathematicians have been attracted by image processing and computer vision in recent years. This has been triggered by mathematically well-founded methods using e.g. wavelets or nonlinear partial differential equations. The goal of the present paper is to give an introduction to a subarea of this field, namely methods that are based on nonlinear diffusion techniques.

This field has evolved in a very fruitful way. It is closely connected to a specific kind of multiscale analysis called scale-space [23, 32], and it has first been used for image smoothing with simultaneous edge enhancement [26]. Later on, close connections to regularization methods have been discovered [29], and related nonlinear methods have also entered computer vision fields such as motion analysis in image sequences [8] or interactive segmentation [4, 20]. In this paper we shall learn about the basic ideas behind these methods, but also about their theoretical foundation and their adequate numerical realization.

In this context we will also discuss the specific requirements for adequate numerical schemes in image processing or computer vision. Among the variety of

Received January 10, 2001.

2000 *Mathematics Subject Classification*. Primary 35-K35, 65-M06, 68-W10, 94-A08.

Key words and phrases. Nonlinear diffusion, variational methods, image processing, computer vision, finite difference methods, parallel algorithms, mean curvature motion.

numerical methods that fulfill these requirements, we focus on a specific class of splitting-based finite difference schemes. These semi-implicit schemes differ from their classical counterparts by the fact that they use additive operator splittings (AOS) instead of multiplicative ones. It will be shown that these AOS schemes are simple and efficient, do not require additional parameters, inherit important properties from the continuous equations, and are widely applicable.

The paper is organized as follows: Section 2 gives an introduction to nonlinear diffusion filtering, while Section 3 describes its relation to regularization methods. In Section 4, nonlinear diffusion is used for analysing motion in image sequences, and Section 5 shows how diffusion-like ideas can be used for interactive segmentation. Each of these sections explains the main ideas, the theoretical foundation of the method, and an appropriate numerical realization in terms of AOS schemes. While sections 2–4 survey work that has been published elsewhere, a novel AOS scheme for mean curvature motion and geodesic active contours is introduced in Section 5.

Related work. In view of the large amount of publications in this area, we have to refer the reader to some recent collections and books in order to obtain a more detailed overview of the state-of-the-art in diffusion-based image processing [5, 23, 32, 34]. Compared to this large number of publications, however, the number of papers dealing with numerical aspects of diffusion filtering is still relatively small. Since the pixel structure of digital images provides a natural discretization on a fixed rectangular grid, it is not surprising that often finite difference methods are used in the image processing community. For simplicity reasons, explicit schemes are still very common, but absolutely stable semi-implicit schemes [6, 13, 39] are becoming more and more popular. Alternatives to finite differences include finite element methods [3, 19, 27, 30], wavelets [10, 11], finite and complementary volume schemes [13], pseudospectral approaches [11], lattice Boltzmann methods [17], and stochastic simulations [28].

2. NONLINEAR DIFFUSION FILTERING

2.1. Basic Idea

Nonlinear diffusion filtering goes back to Perona and Malik [26]. Although their method in its original formulation is regarded to be ill-posed, it has triggered a lot of research; see [33, 34] for overviews. In the following we shall be concerned with one of its earliest regularizations that is due to Catté, Lions, Morel, and Coll [6].

Let $\Omega := (0, a_1) \times \cdots \times (0, a_m)$ be our image domain in \mathbb{R}^m and consider a (scalar) image $f(x) \in L^\infty(\Omega)$. Then a filtered image $u(x, t)$ of $f(x)$ is calculated by solving a nonlinear diffusion equation with the original image as initial state, and homogeneous Neumann boundary conditions:

$$(1) \quad \partial_t u = \operatorname{div} (g(|\nabla u_\sigma|^2) \nabla u) \quad \text{on } \Omega \times (0, \infty),$$

$$(2) \quad u(x, 0) = f(x) \quad \text{on } \Omega,$$

$$(3) \quad \partial_n u = 0 \quad \text{on } \partial\Omega \times (0, \infty),$$

where n denotes the normal to the image boundary $\partial\Omega$.

The “time” t is a scale parameter: larger values lead to simpler image representations. In order to reduce smoothing at edges, the diffusivity g is chosen as a decreasing function of the edge detector $|\nabla u_\sigma|^2$, where ∇u_σ is the gradient of a Gaussian-smoothed version of u :

$$(4) \quad \nabla u_\sigma := \nabla(K_\sigma * u),$$

$$(5) \quad K_\sigma := \frac{1}{(2\pi\sigma^2)^{m/2}} \exp\left(-\frac{|x|^2}{2\sigma^2}\right).$$

We use the diffusivity

$$(6) \quad g(s^2) := \begin{cases} 1 & (s^2 = 0) \\ 1 - \exp\left(\frac{-c}{(s/\lambda)^8}\right) & (s^2 > 0). \end{cases}$$

For such rapidly decreasing diffusivities, smoothing on both sides of an edge is much stronger than smoothing across it. This selective smoothing process prefers intraregional smoothing to interregional blurring. One can ensure that the flux $\Phi(s) := sg(s^2)$ is increasing for $|s| \leq \lambda$ and decreasing for $|s| > \lambda$ by choosing $c \approx 3.315$. Thus, λ is a contrast parameter separating low-contrast regions with (smoothing) forward diffusion from high-contrast locations where backward diffusion may enhance edges [26]. Other choices of diffusivities are possible as well, but experiments indicated that (6) may lead to more segmentation-like results than the functions used in [26].

Figure 1 shows an application of image restoration by means of such a forward-backward diffusion filter. A mammogram is denoised in such a way that the diagnostically relevant microcalcifications become much better visible.

2.2. Theoretical Foundation

2.2.1. Continuous Formulation. The preceding nonlinear diffusion filter belongs to a much larger filter class for which useful theoretical properties can be established. In particular it is possible to replace the scalar-valued diffusivity g by a smooth matrix-valued function D that remains uniformly positive definite as long as its argument is bounded. This allows for more flexible nonlinear diffusion models [34]. For such a class the following properties can be established.

- (a) (Well-posedness and smoothness results)
There exists a unique solution $u(x, t)$ in the distributional sense which is in $C^\infty(\bar{\Omega} \times (0, \infty))$ and depends continuously on f with respect to the $L^2(\Omega)$ norm.
- (b) (Extremum principle)
Let $a := \inf_\Omega f$ and $b := \sup_\Omega f$. Then, $a \leq u(x, t) \leq b$ on $\Omega \times [0, \infty)$.

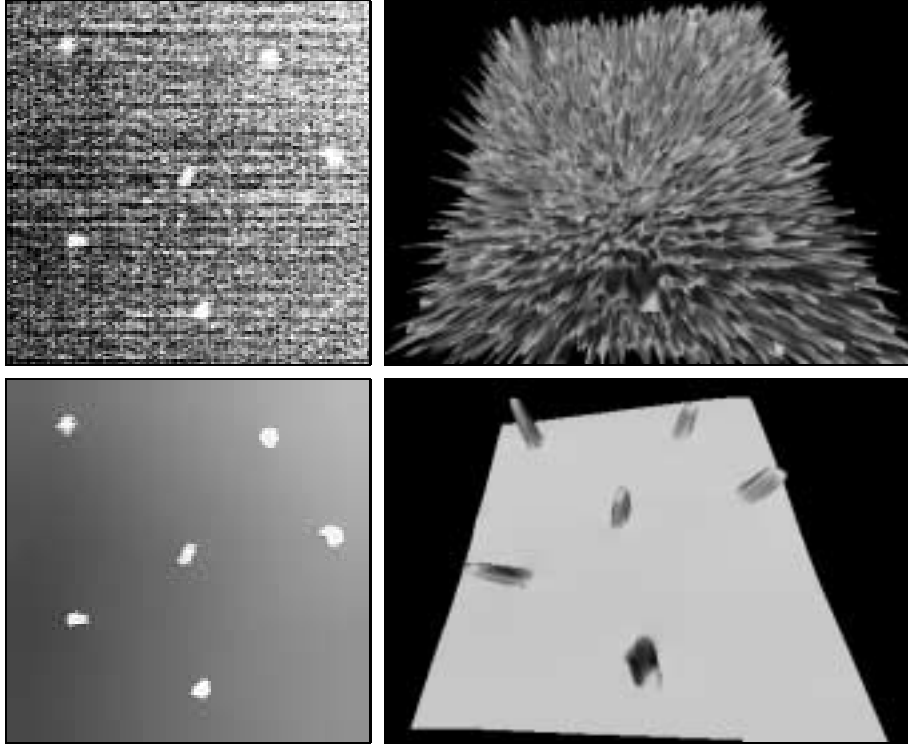


Figure 1. (a) TOP LEFT: Mammogram with six microcalcifications, $\Omega = (0, 128)^2$. (b) TOP RIGHT: 3D plot of (a), where the graph of f is regarded as a surface in \mathbb{R}^3 . (c) BOTTOM LEFT: Nonlinear diffusion filtering of (a) ($\sigma=1$, $\lambda=7.5$, $t=128$). (d) BOTTOM RIGHT: 3D plot of (c).

(c) (Average grey level invariance)

The average grey level $\mu := \frac{1}{|\Omega|} \int_{\Omega} f(x) dx$ is not affected by nonlinear diffusion filtering: $\frac{1}{|\Omega|} \int_{\Omega} u(x, t) dx = \mu$ for all $t > 0$.

(d) (Lyapunov functionals)

$V(t) := \int_{\Omega} r(u(x, t)) dx$ is a Lyapunov function for all convex $r \in C^2[a, b]$:

$V(t)$ is decreasing and bounded from below by $\int_{\Omega} r(\mu) dx$.

(e) (Convergence to a constant steady state)

$\lim_{t \rightarrow \infty} u(x, t) = \mu$ in $L^p(\Omega)$, $1 \leq p < \infty$.

The existence, uniqueness and regularity proof is due to [6], the other results are proved in [34].

Continuous dependence of the solution on the initial image is of significant practical importance, since it guarantees stability under perturbations. This is relevant when considering stereo images, image sequences or slices from medical CT or MR sequences, since we know that similar images remain similar after filtering.

Hummel [15] has shown that, for a large class of linear and nonlinear parabolic operators, extremum principles imply that no new level sets can be created that are absent at smaller scales $t > 0$. This so-called **causality** property allows to trace back structures in time (e.g. in order to improve their localization). It is important in many computer vision applications.

Average grey level invariance is a property which distinguishes nonlinear diffusion filtering from other PDE-based image processing techniques such as mean curvature motion [2]. The latter one is not in divergence form and, thus, can not be conservative. Average grey level invariance is required in some segmentation algorithms such as the Hyperstack [24].

Lyapunov functionals are of theoretical importance, as they allow to prove that – in spite of its image enhancing qualities – our filter class consists of smoothing transformations: Indeed, the special choices $r(s) := |s|^p$, $r(s) := (s - \mu)^{2n}$ and $r(s) := s \ln s$, respectively, imply that all L^p norms with $2 \leq p \leq \infty$ are decreasing (e.g. the energy $\|u(t)\|_{L^2(\Omega)}^2$), all even central moments are decreasing (e.g. the variance), and the entropy $S[u(t)] := -\int_{\Omega} u(x,t) \ln(u(x,t)) dx$, a measure of uncertainty and missing information, is increasing with respect to t . Thus, in spite of the fact that our filters may act image enhancing, their global smoothing properties in terms of Lyapunov functionals can be interpreted in a deterministic, stochastic, and information-theoretic manner.

The result (e) tells us that, for $t \rightarrow \infty$, diffusion filtering tends to the most global image representation that is possible: a constant image with the same average grey level as f .

A continuous family $\{u(t) \mid t \geq 0\}$ of simplified versions of $f = u(0)$ with properties like the ones above is called a **scale-space representation**. Scale-spaces have turned out to be useful image processing and computer vision techniques with many applications [23, 32].

2.2.2. Semidiscrete and Discrete Formulations. The preceding theoretical framework yielded several properties that are desirable from an image processing viewpoint. Since digital images are discretized on a regular pixel grid, however, the natural question arises whether these properties are still preserved for suitable numerical approximations. We would thus need semidiscrete and discrete theories that guarantee the same properties.

Such a framework has been developed in [34], both for the spatially discrete and for the fully discrete case when finite differences are used. In this setting, semidiscrete filters (discrete in space and continuous in time) are given by a coupled system of ordinary differential equations, while fully discrete methods may lead to matrix-vector multiplications where the matrix depends nonlinearly on the evolving image.

Table 1 gives an overview of the requirements which are needed in order that well-posedness properties, average grey value invariance, causality in terms of an extremum principle and Lyapunov functionals, and convergence to a constant steady-state are inherited from the continuous setting. We observe that the requirements belong to five categories: smoothness, symmetry, conservation,

nonnegativity and connectivity requirements. These criteria are easy to check for many discretizations.

requirement	continuous $\partial_t u = \operatorname{div}(D\nabla u)$ $u(x, 0) = f(x)$	semidiscrete $\frac{du}{dt} = A(u)u$ $u(0) = f$	discrete $u^{k+1} = Q(u^k)u^k$ $u^0 = f$
smoothness	$D \in C^\infty$	A Lipschitz-continuous	Q continuous
symmetry	D symmetric	A symmetric	Q symmetric
conservation	divergence form; $\langle D\nabla u, n \rangle = 0$	$\sum_i a_{ij} = 0$	$\sum_i q_{ij} = 1$
nonnegativity	positive semidefinite	nonnegative off-diagonals	nonnegative elements
connectivity	uniformly positive definite	A irreducible	Q irreducible; pos. diagonal

Table 1. Requirements for continuous, semidiscrete and fully discrete nonlinear diffusion scale-spaces. In the continuous case, u is a function of space and time, in the semidiscrete case it is a time-dependent vector, and in the fully discrete case, u^k is a vector. From [34].

It should be noted that this table provides design criteria for reliable algorithms. Criteria that guarantee a discrete extremum principle, for instance, constitute strong stability properties. The table also shows an important difference between image processing and other fields of scientific computing. In other fields, a diffusion equation is motivated from some underlying physical problem. Hence, a good numerical method aims at approximating it as closely as possible. This may result e.g. in high-order methods and sophisticated error estimators. In image processing there is no physical problem behind the model. Thus, one might be more interested in methods that inherit all qualitative properties of a continuous model than in highly precise, but possibly oscillating schemes.

It should also be noted that our discrete scale-space framework is not necessarily limited to finite difference methods, as it is well known that e.g. finite volume schemes on a regular grid may lead to the same algorithms. On the other hand, it is worth mentioning that this framework can only give **sufficient** criteria for well-founded and stable discrete processes. These criteria are not necessarily the only way to go, as one can see e.g. from the theoretically well-investigated alternatives in [13, 19, 30].

2.3. Adequate Numerical Schemes

2.3.1. Classical Semi-Implicit Schemes. Let us now consider finite difference approximations to the m -dimensional diffusion filter of Catté et al. [6]. A discrete m -dimensional image can be regarded as a vector $f \in \mathbb{R}^N$, whose components f_i , $i \in \{1, \dots, N\}$ display the grey values at the pixels. Pixel i represents the location x_i . Let h_l denote the grid size in the l direction. We consider discrete

times $t_k := k\tau$, where $k \in \mathbb{N}_0$ and τ is the time step size. By u_i^k and g_i^k we denote approximations to $u(x_i, t_k)$ and $g(|\nabla u_\sigma(x_i, t_k)|^2)$, respectively, where the gradient is replaced by central differences.

A semi-implicit (linear implicit) discretization of the diffusion equation with reflecting boundary conditions is given by

$$(7) \quad \frac{u_i^{k+1} - u_i^k}{\tau} = \sum_{l=1}^m \sum_{j \in \mathcal{N}_l(i)} \frac{g_j^k + g_i^k}{2h_l^2} (u_j^{k+1} - u_i^{k+1}).$$

where $\mathcal{N}_l(i)$ consists of the two neighbours of pixel i along the l direction (boundary pixels may have only one neighbour). In vector-matrix notation this becomes

$$(8) \quad \frac{u^{k+1} - u^k}{\tau} = \sum_{l=1}^m A_l(u^k) u^{k+1}.$$

A_l describes the diffusive interaction in l direction. This scheme does not give the solution u^{k+1} directly: it requires to solve a linear system first. Its solution is formally given by

$$(9) \quad u^{k+1} = \left(I - \tau \sum_{l=1}^m A_l(u^k) \right)^{-1} u^k.$$

In [34] it is shown that this scheme satisfies all discrete scale-space requirements for all time step sizes $\tau > 0$. This absolute stability shows in particular that one does not have to consider numerically more expensive fully implicit schemes.

How expensive is it to solve the linear system? In the 1-D case the system matrix is tridiagonal and diagonally dominant. Here a simple Gaussian algorithm for tridiagonal systems solves the problem in linear complexity. For dimensions $m \geq 2$, however, the matrix may reveal a much larger bandwidth. Applying direct algorithms such as Gaussian elimination would destroy the zeros within the band and would lead to an immense storage and computation effort. Classical iterative algorithms become slow for large τ , since this increases the condition number of the system matrix. Hence, it would be natural to consider e.g. multigrid methods [1] whose convergence can be independent of the condition number, or preconditioned conjugate gradient methods [13, 27]. In the following we shall focus on a splitting-based alternative. It is simple to implement and does not require to specify any additional parameters. This may make it attractive in a number of image processing and computer vision applications.

2.3.2. AOS Schemes. Let us now consider a modification of (9), namely the **additive operator splitting (AOS) scheme** [39]

$$(10) \quad u^{k+1} = \frac{1}{m} \sum_{l=1}^m \left(I - m\tau A_l(u^k) \right)^{-1} u^k.$$

The operators $B_l(u^k) := I - m\tau A_l(u^k)$ describe one-dimensional diffusion processes along the x_l axes. Under a consecutive pixel numbering along the direction l they

come down to strictly diagonally dominant tridiagonal linear systems which can be solved in linear complexity with a simple Gaussian algorithm.

It should be noted that (10) has the same first-order Taylor expansion in τ as the semi-implicit scheme: both methods are $O(\tau + h_1^2 + \dots + h_m^2)$ approximations to the continuous equation.

Moreover, since (10) is an **additive** splitting, all coordinate axes are treated in exactly the same manner. This is in contrast to conventional splitting techniques from the literature such as ADI methods, D'yakonov splitting or LOD techniques [21]: they are **multiplicative** and may produce different results in the nonlinear setting if the image is rotated by 90 degrees, since the operators do not commute. In general, they also produce nonsymmetric system matrices, for which the discrete scale-space framework from Table 1 is not applicable.

The AOS scheme, however, does not require commuting operators, and it satisfies the discrete scale-space framework for all time step sizes [39]. As a consequence, it preserves the average grey level μ , satisfies a causality property in terms of a maximum–minimum principle, possesses the desired class of Lyapunov sequences and converges to a constant steady state.

In practice, it makes of course not much sense to use extremely large time steps, since this leads to poor rotation invariance, as splitting effects become visible. Evaluations have shown that for $h_1 = h_2 = 1$ a step size of $\tau = 5$ is a good compromise between accuracy and efficiency [39]. Many nonlinear diffusion problems require only the elimination of noise and some small-scale details. Often this can be accomplished with no more than 5 discrete time steps. This requires about 0.3 CPU seconds for an image with 256×256 pixels on a 700 MHz PC. For many applications this is sufficiently fast.

In case one is interested in a further speed-up, one should notice that AOS schemes are well-suited for parallel computing as they possess two granularities of parallelism:

- Coarse grain parallelism: Diffusion in different directions can be performed simultaneously on different processors.
- Mid grain parallelism: 1D diffusions along the same direction decouple as well.

Motivated from our encouraging results with AOS schemes on a shared memory machine [36], we are currently studying their behaviour on architectures with distributed memory such as system area networks with low latency communication.

3. REGULARIZATION METHODS

3.1. Basic Idea and Theoretical Foundation

Regularization methods constitute an interesting alternative to nonlinear diffusion filters. Typical variational methods for image restoration (such as [7], [9], [16], [25], [30]) obtain a filtered version of some degraded image f as the minimizer u_α

of

$$(11) \quad E_f(u) := \int_{\Omega} \left((u-f)^2 + \alpha \Psi(|\nabla u|^2) \right) dx.$$

The first summand encourages similarity between the restored image and the original one, while the second summand rewards smoothness. The smoothness weight $\alpha > 0$ is called regularization parameter. In our case, the regularizer Ψ is supposed to satisfy the following conditions:

- $\Psi(\cdot)$ is continuous for any compact $K \subseteq [0, \infty)$.
- $\Psi(|\cdot|^2)$ is convex from \mathbb{R}^m to \mathbb{R} .
- $\Psi(\cdot)$ is increasing in $[0, \infty)$.
- There exists a constant $\varepsilon > 0$ with $\Psi(s^2) \geq \varepsilon s^2$.

One example is given by

$$(12) \quad \Psi(s^2) = \lambda^2 \sqrt{1 + s^2/\lambda^2} + \varepsilon s^2.$$

For this class of regularization methods one can establish a similar well-posedness and scale-space framework as for nonlinear diffusion filtering if one considers the regularization parameter α as scale. In [29] the following properties have been proved:

- (a) (Well-posedness and regularity)
Let $f \in L^\infty(\Omega)$. Then the functional (11) has a unique minimizer u_α in the Sobolev space $H^1(\Omega)$. Moreover, $u_\alpha \in H^2(\Omega)$ and $\|u_\alpha\|_{L^2(\Omega)}$ depends continuously on α .
- (b) (Extremum principle)
Let $a := \inf_{\Omega} f$ and $b := \sup_{\Omega} f$. Then, $a \leq u_\alpha(x) \leq b$ on Ω .
- (c) (Average grey level invariance)
The average grey level $\mu := \frac{1}{|\Omega|} \int_{\Omega} f(x) dx$ remains constant under regularization: $\frac{1}{|\Omega|} \int_{\Omega} u_\alpha(x) dx = \mu$.
- (d) (Lyapunov functionals)
 $V(\alpha) := \int_{\Omega} r(u_\alpha(x)) dx$ is a Lyapunov functional for all $r \in C^2[a, b]$ with $r'' \geq 0$: $V(\alpha) \leq V(0)$ for all $\alpha \geq 0$ and $V(\alpha) \geq \int_{\Omega} r(\mu) dx$.
- (e) (Convergence to a constant image for $\alpha \rightarrow \infty$)
If $m = 2$, then $\lim_{\alpha \rightarrow \infty} \|u_\alpha - \mu\|_{L^p(\Omega)} = 0$ for any $p \in [1, \infty)$.

Let us now give an intuitive reason for this large amount of structural similarities between diffusion filters and regularization methods. If Ψ is differentiable, then the minimizer of $E_f(u)$ satisfies the Euler-Lagrange equation

$$(13) \quad \frac{u-f}{\alpha} = \operatorname{div} \left(\Psi'(|\nabla u|^2) \nabla u \right).$$

This can be regarded as a fully implicit time discretization of the diffusion filter

$$(14) \quad \partial_t u = \operatorname{div} \left(\Psi'(|\nabla u|^2) \nabla u \right)$$

with one discrete time step of size α . One may thus regard our well-posedness and scale-space framework for regularization methods as a time-discrete framework for diffusion filtering. This would constitute another column in Table 1.

It should be noted, however, that we have restricted ourselves to convex regularizers Ψ . In this case the flux function $\Psi'(s^2)$ is always increasing. This implies that there is no contrast enhancement in a similar way as for forward-backward diffusion filters. Nevertheless, since the diffusivity $\Psi'(|\nabla u|^2)$ is decreasing in $|\nabla u|^2$, smoothing at edges is reduced and discontinuities are better preserved than with linear smoothing methods.

3.2. Numerical Approximation

From the discussion in the last section it follows that one may use any diffusion algorithm in order to approximate a regularization method. All one has to do is to use the regularization parameter as stopping time.

If one wants to have a more accurate approximation, an alternative way to use diffusion techniques would be to discretize the steepest descent equation of (11),

$$(15) \quad \partial_t u = \operatorname{div} \left(\Psi'(|\nabla u|^2) \nabla u \right) + \frac{1}{\alpha} (f - u),$$

and extract the desired regularization from its steady state ($t \rightarrow \infty$). In matrix-vector notation a semi-implicit discretization of this diffusion-reaction equation is given by

$$(16) \quad \frac{u^{k+1} - u^k}{\tau} = \sum_{l=1}^m A_l(u^k) u^{k+1} + \frac{1}{\alpha} (f - u^{k+1}).$$

Solving for u^{k+1} yields

$$(17) \quad u^{k+1} = \left(I - \frac{\alpha\tau}{\alpha + \tau} \sum_{l=1}^m A_l(u^k) \right)^{-1} \frac{\alpha u^k + \tau f}{\alpha + \tau}.$$

In analogy to the previous section we may replace this scheme by its AOS approximation

$$(18) \quad u^{k+1} = \frac{1}{m} \sum_{l=1}^m \left(I - \frac{m\alpha\tau}{\alpha + \tau} A_l(u^k) \right)^{-1} \frac{\alpha u^k + \tau f}{\alpha + \tau}$$

which again leads to simple tridiagonal linear systems of equations.

In contrast to the pure diffusion filter, however, we are now interested in approximating the solution for $t \rightarrow \infty$. In order to speed up the process, we may embed the AOS scheme into a multilevel framework [35]. Experiments have shown that a simple nested iteration strategy with full weighting for restriction and with linear interpolation gives sufficiently fast and accurate results. Hence, the principle is as follows: The original image is downsampled in a pyramid-like manner by applying the convolution mask $[\frac{1}{4}, \frac{1}{2}, \frac{1}{4}]$ in x and y direction until the coarsest resolution is reached. This image is used as initialization at the coarsest level. Then a fixed number of AOS iterations is applied, and the result is linearly interpolated to the next higher level where it serves as initialization. This is repeated until the

finest level is reached again. Figure 2 illustrates this approach. Regularizing a 256^2 image on a 700 MHz PC with 5 time steps per level requires about 0.3 CPU seconds.



Figure 2. (a) TOP: Restriction of a noisy test image. (b) BOTTOM: Regularized by an AOS scheme embedded in a nested iteration strategy. From [35].

4. OPTIC FLOW ESTIMATION

Let us now investigate the use of nonlinear diffusion processes in the context of image sequence analysis. One of the main goals of image sequence analysis is the recovery of the so-called **optic flow** field. Optic flow describes the apparent motion of structures in the image plane. It can be used in a large variety of

applications ranging from the recovery of motion parameters in robotics to the design of efficient algorithms for second generation video compression.

In the following we consider an image sequence $f(x, y, z)$ where $(x, y) \in \Omega$ denotes the location and $z \in [0, Z]$ is the time. We are looking for the optic flow field $\begin{pmatrix} u(x, y, z) \\ v(x, y, z) \end{pmatrix}$ which describes the correspondence of image structures at different times. Variational methods constitute one possibility to solve the optic flow problem; see e.g. [8, 14, 22, 37]. In [38] a method is considered which is based on the following two assumptions:

1. Image structures do not change their grey value over time. Therefore, along their path $(x(z), y(z))$ one obtains

$$(19) \quad 0 = \frac{df(x(z), y(z), z)}{dz} = f_x u + f_y v + f_z.$$

2. As second assumption we impose a spatio-temporal smoothness constraint:

$$(20) \quad \int_{\Omega \times [0, Z]} \Psi (|\nabla_3 u|^2 + |\nabla_3 v|^2) \, dx \, dy \, dz \quad \text{is "small",}$$

where $\nabla_3 := (\partial_x, \partial_y, \partial_z)^T$ and Ψ is a regularizer as in the previous section.

Combining these two constraints in a single energy functional, one can obtain the optic flow as a minimizer of

$$(21) \quad E_f(u, v) := \int_{\Omega \times [0, Z]} \left((f_x u + f_y v + f_z)^2 + \alpha \Psi (|\nabla_3 u|^2 + |\nabla_3 v|^2) \right) \, dx \, dy \, dz.$$

This functional can be regarded as a special representative of a much larger class of optic flow functionals for which one can establish general well-posedness results in $H^1(\Omega \times (0, T)) \times H^1(\Omega \times (0, T))$. For more details the reader is referred to [37].

The steepest descent equations for (21) with a differentiable regularizer Ψ are

$$(22) \quad u_t = \nabla_3 \cdot (\Psi' (|\nabla_3 u|^2 + |\nabla_3 v|^2) \nabla_3 u) - \frac{1}{\alpha} f_x (f_x u + f_y v + f_z),$$

$$(23) \quad v_t = \nabla_3 \cdot (\Psi' (|\nabla_3 u|^2 + |\nabla_3 v|^2) \nabla_3 v) - \frac{1}{\alpha} f_y (f_x u + f_y v + f_z).$$

This is a coupled three-dimensional diffusion–reaction system. It may be treated numerically in the same way as the regularization methods from the last section. In matrix-vector notation, the resulting AOS scheme is given by

$$(24) \quad u^{k+1} = \frac{1}{3} \sum_{l=1}^3 \left(I + \frac{3\tau}{\alpha} f_x^2 I - 3\tau A_l(u^k, v^k) \right)^{-1} \left(u^k - \frac{\tau}{\alpha} f_x (f_y v^k + f_z) \right),$$

$$(25) \quad v^{k+1} = \frac{1}{3} \sum_{l=1}^3 \left(I + \frac{3\tau}{\alpha} f_y^2 I - 3\tau A_l(u^k, v^k) \right)^{-1} \left(v^k - \frac{\tau}{\alpha} f_y (f_x u^k + f_z) \right).$$

Since the continuous and discrete processes are globally convergent for convex diffusivities, the specific choice of the initial values is not very important. In our experiments the flow is initialized with zero. Figure 3 shows an example. We

can see that the recovered optic flow field gives a quite realistic description of the person's movement towards the camera.



Figure 3. (a) LEFT: One frame of a hallway sequence with $256 \times 256 \times 16$ pixels. A person is approaching the camera. (b) MIDDLE: Detail. (c) RIGHT: Computed optic flow. From [38].

5. GEODESIC ACTIVE CONTOURS

5.1. Basic Idea and Theoretical Properties

Active contours [18] play an important role in interactive image segmentation, in particular for medical applications. The basic idea is that the user specifies an initial guess of an interesting contour (organ, tumour, ...). Then this contour is moved by image-driven forces to the edges of the desired object.

So-called geodesic active contour models [4, 20] achieve this by applying a specific kind of level set ideas [31]. In its simplest form, a geodesic active contour model consists of the following steps. One embeds the user-specified initial curve $C_0(s)$ as a zero level curve into a function $u_0: \mathbb{R}^2 \rightarrow \mathbb{R}$, for instance by using the distance transformation. Then u_0 is evolved under a PDE which includes knowledge about the original image f :

$$(26) \quad \partial_t u = |\nabla u| \operatorname{div} \left(g(|\nabla f_\sigma|^2) \frac{\nabla u}{|\nabla u|} \right),$$

where g inhibits evolution at edges of f . One may choose decreasing functions such as (6). Experiments indicate that, in general, (26) will have nontrivial steady states. The evolution is stopped at some time T , when the process does hardly alter anymore, and the final contour C is extracted as the zero level curve of $u(x, T)$. Figure 4 gives an example of such a geodesic active contour evolution. It can be interpreted as a curve evolution that follows a modified mean curvature motion.

The theoretical analysis from [4, 20] shows that the initial value problem has a unique viscosity solution $u \in L^\infty(0, T; W^{1,\infty}(\mathbb{R}^2)) \cap C([0, \infty) \times \mathbb{R}^2)$ for initial data $u_0 \in C(\mathbb{R}^2) \cap W^{1,\infty}(\mathbb{R}^2)$. This solution satisfies an extremum principle and depends continuously on the initial data with respect to the L^∞ norm.



Figure 4. Temporal evolution of a geodesic active contour superimposed on the original image ($\Omega = (0, 256)^2$, $\lambda = 5$, $\sigma = 1$). FROM LEFT TO RIGHT: $t = 0, 1500, 7500$. Larger values for t do not alter the result .

5.2. Numerical Approximation

Next we present a novel scheme for the geodesic active contour model. Although (26) is not a diffusion process in a strict sense – it cannot be written in divergence form – one may use similar techniques as before.

The case $\nabla u = 0$ can be treated numerically by imposing no changes at these points. Several modifications are possible, but this case is less important since one is interested in steady states where the embedded level set does not vanish. Let us therefore consider the case where $\nabla u \neq 0$ in some pixel i . Here straightforward finite difference implementations would give rise to problems when ∇u vanishes in the 4-neighbourhood $\mathcal{N}(i)$ of i . These problems do not appear if one uses a finite difference scheme with **harmonic** averaging. In its semi-implicit formulation such a scheme reads

$$(27) \quad \frac{u_i^{k+1} - u_i^k}{\tau} = |\nabla u|_i^k \sum_{j \in \mathcal{N}(i)} \frac{2}{\left(\frac{|\nabla u|}{g}\right)_j^k + \left(\frac{|\nabla u|}{g}\right)_i^k} \frac{u_j^{k+1} - u_i^{k+1}}{h^2}.$$

Note that the denominator cannot vanish in this scheme. One can also verify that such a scheme is absolutely stable, since it satisfies the discrete extremum principle

$$(28) \quad \min_i u_{0,i} \leq u_j^k \leq \max_i u_{0,i}$$

for all j and for all $k > 0$. An AOS variant of this scheme can be constructed in exactly the same manner as in Section 2. The only difference is that $A_l(u^k) u^{k+1}$ is now a semi-implicit discretization of $|\nabla u| \partial_{x_l} (g \nabla u / |\nabla u|)$ instead of $\partial_{x_l} (g \nabla u)$. It may be accelerated by embedding it in a multilevel framework as is described in Section 3.2. The AOS scheme for geodesic active contours also inherits absolute

stability from (27), while a simple explicit variant of (27) would only be stable for $\tau \leq h^2/8$.

It should be mentioned that this AOS strategy is not the only AOS approach that has been proposed for geodesic active contours. In [12], Goldenberg et al. present a method that requires to apply a distance transformation in each iteration [31]. This is done in order to obtain $|\nabla u| = 1$ such that (26) becomes the diffusion process

$$(29) \quad \partial_t u = \operatorname{div} (g(|\nabla f_\sigma|^2) \nabla u)$$

for which the standard AOS from Section 2 is used. Since our method does not require any time-consuming distance transformation in each iteration step, it is simpler and computationally more efficient.

5.3. Evaluation in Case of Mean Curvature Motion

It is obvious that the preceding AOS-based harmonic averaging scheme can also be used for computing mean curvature motion for the case $g = 1$. In this situation a simple numerical evaluation is possible: Since it is well-known that a disk-shaped level set with area $S(0)$ shrinks under mean curvature motion such that

$$(30) \quad S(t) = S(0) - 2\pi t,$$

simple accuracy evaluations are possible. To this end we used a distance transformation of some disk-shaped initial image and considered the evolution of a level set with an initial area of 24845 pixels. Table 2 shows the area errors for different time step sizes τ and two stopping times. We observe that for $\tau \leq 5$, the accuracy is sufficiently high for typical image processing applications. Figure 5 demonstrates that in this case no violations regarding rotational invariance are visible.

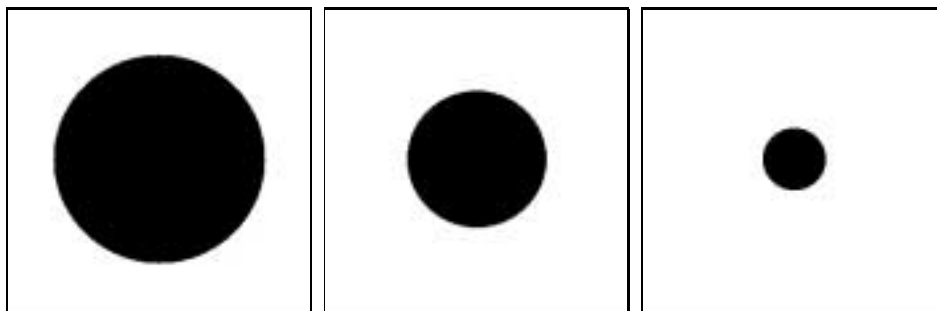


Figure 5. Temporal evolution of a disk-shaped level set under mean curvature motion. The results have been obtained using an AOS-based semi-implicit scheme with harmonic averaging and step size $\tau = 5$. FROM LEFT TO RIGHT: $t = 0, 2250, 3600$.

step size τ	stopping time $T = 2250$	stopping time $T = 3600$
0.5	-0.27 %	-0.60 %
1	-0.26 %	-0.88 %
2	-0.27 %	-0.88 %
5	-0.34 %	-1.73 %
10	-5.18 %	51.20 %

Table 2. Area errors for the evolution of a disk-shaped area of 24845 pixels under mean curvature motion using an AOS-based semi-implicit scheme with harmonic averaging. The pixels have size 1 in each direction.

REFERENCES

1. Acton S. T., *Multigrid anisotropic diffusion*, IEEE Transactions on Image Processing **7** (1998), 280–291.
2. Alvarez L., Lions P.-L. and Morel J.-M., *Image selective smoothing and edge detection by nonlinear diffusion. II*, SIAM Journal on Numerical Analysis **29** (1992), 845–866.
3. Bänsch E. and Mikula K., *A coarsening finite element strategy in image selective smoothing*, Computation and Visualization in Science **1** (1997), 53–61.
4. Caselles V., Kimmel R. and Sapiro G., *Geodesic active contours*, International Journal of Computer Vision **22** (1997), 61–79.
5. Caselles V., Morel J.-M., Sapiro G. and Tannenbaum A., eds., Special Issue on Partial Differential Equations and Geometry-Driven Diffusion in Image Processing and Analysis, Vol. **7**(3) of IEEE Transactions on Image Processing, IEEE Signal Processing Society Press, Mar. 1998.
6. Catté F., Lions P.-L., Morel J.-M. and Coll T., *Image selective smoothing and edge detection by nonlinear diffusion*, SIAM Journal on Numerical Analysis **32** (1992), 1895–1909.
7. Charbonnier P., Blanc-Féraud L., Aubert G. and Barlaud M., *Two deterministic half-quadratic regularization algorithms for computed imaging*, In Proc. 1994 IEEE International Conference on Image Processing, Vol. **2**, Austin, TX, IEEE Computer Society Press, pp. 168–172, Nov. 1994.
8. Cohen I., *Nonlinear variational method for optical flow computation*, In Proc. Eighth Scandinavian Conference on Image Analysis, Vol. **1**, Tromsø, Norway, pp. 523–530, May 1993.
9. Deriche R. and Faugeras O., *Les EDP en traitement des images et vision par ordinateur*, Traitement du Signal **13** (1996), pp. 551–577, Numéro Spécial.
10. Fontaine F. L. and Basu S., *Wavelet-based solution to anisotropic diffusion equation for edge detection*, International Journal of Imaging Systems and Technology **9** (1998), 356–368.
11. Fröhlich J. and Weickert J., *Image processing using a wavelet algorithm for nonlinear diffusion*, Tech. Rep. 104, Laboratory of Technomathematics, University of Kaiserslautern, Germany, Mar. 1994.
12. Goldenberg R., Kimmel R., Rivlin E. and Rudzsky M., *Fast geodesic active contours*, in Scale-Space Theories in Computer Vision (M. Nielsen, P. Johansen, O. F. Olsen and J. Weickert, eds.), Vol. **1682** of Lecture Notes in Computer Science, pp. 34–45, Springer, Berlin, 1999.
13. Handlovičová A., Mikula K. and Sgallari F., *Variational numerical methods for solving diffusion equation arising in image processing*, Journal of Visual Communication and Image Representation, (2001), to appear.
14. Horn B. and Schunck B., *Determining optical flow*, Artificial Intelligence **17** (1981), 185–203.
15. Hummel R. A., *Representations based on zero-crossings in scale space*, in Proc. 1986 IEEE Computer Society Conference on Computer Vision and Pattern Recognition, Miami Beach, FL, June 1986, IEEE Computer Society Press, pp. 204–209.

16. Ito K. and Kunisch K., *An active set strategy based on the augmented Lagrangian formulation for image restoration*, RAIRO Mathematical Models and Numerical Analysis **33** (1999), 1–21.
17. Jawerth B., Lin P. and Sinzinger E., *Lattice Boltzmann models for anisotropic diffusion of images*, Journal of Mathematical Imaging and Vision **11** (1999), 231–237.
18. Kass M., Witkin A. and Terzopoulos D., *Snakes: Active contour models*, International Journal of Computer Vision **1** (1988), 321–331.
19. Kačur J. and Mikula K., *Solution of nonlinear diffusion appearing in image smoothing and edge detection*, Applied Numerical Mathematics **17** (1995), 47–59.
20. Kichenassamy S., Kumar A., Olver P., Tannenbaum A. and Yezzi A., *Conformal curvature flows: from phase transitions to active vision*, Archive for Rational Mechanics and Analysis **134** (1996), 275–301.
21. Marchuk G. I., *Splitting and alternating direction methods*, in Handbook of Numerical Analysis (P. G. Ciarlet and J.-L. Lions, eds.), Vol. **I**, pp. 197–462, North Holland, Amsterdam, 1990.
22. Nagel H.-H. and Enkelmann W., *An investigation of smoothness constraints for the estimation of displacement vector fields from image sequences*, IEEE Transactions on Pattern Analysis and Machine Intelligence **8** (1986), 565–593.
23. Nielsen M., Johansen P., Olsen O. F. and Weickert J., eds., *Scale-Space Theories in Computer Vision*, Vol. **1682** of Lecture Notes in Computer Science, Springer, Berlin, 1999.
24. Niessen W. J., Vincken K. L., Weickert J. and Viergever M. A., *Nonlinear multiscale representations for image segmentation*, Computer Vision and Image Understanding **66** (1997), 233–245.
25. Nordström N., *Biased anisotropic diffusion – a unified regularization and diffusion approach to edge detection*, Image and Vision Computing **8** (1990), 318–327.
26. Perona P. and Malik J., *Scale space and edge detection using anisotropic diffusion*, IEEE Transactions on Pattern Analysis and Machine Intelligence **12** (1990), 629–639.
27. Preußner T. and Rumpf M., *An adaptive finite element method for large scale image processing*, in Scale-Space Theories in Computer Vision (M. Nielsen, P. Johansen, O. F. Olsen, and J. Weickert, eds.), Vol. **1682** of Lecture Notes in Computer Science, pp. 223–234, Springer, Berlin, 1999.
28. Ranjan U. S. and Ramakrishnan K. R., *A stochastic scale space for multiscale image representation*, in Scale-Space Theories in Computer Vision (M. Nielsen, P. Johansen, O. F. Olsen, and J. Weickert, eds.), Vol. **1682** of Lecture Notes in Computer Science, pp. 441–446, Springer, Berlin, 1999.
29. Scherzer O. and Weickert J., *Relations between regularization and diffusion filtering*, Journal of Mathematical Imaging and Vision **12** (2000), 43–63.
30. Schnörr C., *Unique reconstruction of piecewise smooth images by minimizing strictly convex non-quadratic functionals*, Journal of Mathematical Imaging and Vision **4** (1994), 189–198.
31. Sethian J. A., *Level Set Methods and Fast Marching Methods*, Cambridge University Press, Cambridge, UK, 1999.
32. ter Haar Romeny B., Florack L. and Koenderink J., eds., *Scale-Space Theory in Computer Vision*, Vol. **1252** of Lecture Notes in Computer Science, Springer, Berlin, 1997.
33. ter Haar Romeny B. M., ed., *Geometry-Driven Diffusion in Computer Vision*, Vol. **1** of Computational Imaging and Vision, Kluwer, Dordrecht, 1994.
34. Weickert J., *Anisotropic Diffusion in Image Processing*, Teubner, Stuttgart, 1998.
35. ———, *Efficient image segmentation using partial differential equations and morphology*, Pattern Recognition **34** (2001), 1813–1824.
36. Weickert J., Heers J., Schnörr C., Zuiderveld K. J., Scherzer O. and Stiehl H. S., *Fast parallel algorithms for a broad class of nonlinear variational diffusion approaches*, Real-Time Imaging **7** (2001), 31–45.

37. Weickert J. and Schnörr C., *A theoretical framework for convex regularizers in PDE-based computation of image motion*, Tech. Rep. 13/2000, Computer Science Series, University of Mannheim, Germany, June 2000, to appear in International Journal of Computer Vision.
38. ———, *Variational optic flow computation with a spatio-temporal smoothness constraint*, Journal of Mathematical Imaging and Vision **14** (2001), 245–255.
39. Weickert J., ter Haar Romeny B. M. and Viergever M. A., *Efficient and reliable schemes for nonlinear diffusion filtering*, IEEE Transactions on Image Processing **7** (1998), 398–410.

J. Weickert, Computer Vision, Graphics, and Pattern Recognition Group, Department of Mathematics and Computer Science, University of Mannheim, 68131 Mannheim, Germany, *e-mail*: Joachim.Weickert@uni-mannheim.de,
<http://www.cvgrp.uni-mannheim.de/weickert>